The EOS of neutron matter and neutron stars

Stefano Gandolfi

Los Alamos National Laboratory (LANL)

ELBA 2019 - Lepton Interactions with Nucleons and Nuclei
Marciana Marina, June 24-28, 2019.

Los Alamos NATIONAL LABORATORY EST.1943

NUCLEI Nuclear Computational Low-Energy Initiative

U.S. DEPARTMENT OF ENERGY

www.computingnuclei.org

NERSC National Energy Research Scientific Computing Center

U.S. DEPARTMENT OF ENERGY INCITE LEADERSHIP COMPUTING

Neutron stars

Neutron star is a wonderful natural laboratory

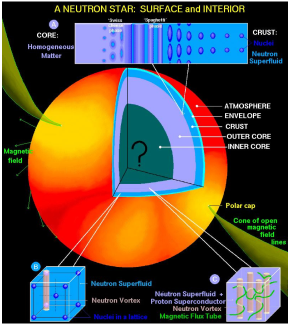

D. Page

- Atmosphere: atomic and plasma physics
- Crust: physics of superfluids (neutrons, vortex), solid state physics (nuclei)
- Inner crust: deformed nuclei, pasta phase
- Outer core: nuclear matter
- Inner core: hyperons? quark matter? π or K condensates?

Gravitational waves:

- Mass and Radius
- Tidal deformability
- ...

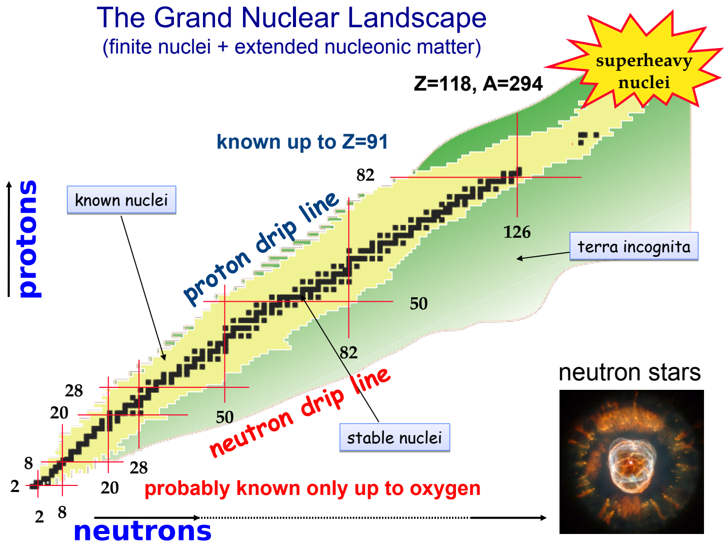

W. Nazarewicz

Outline

- The model and the method
- Equation of state of neutron matter
- Nuclear EOS, radius of neutron stars, and nuclear symmetry energy
- High density EOS, speed of sound, maximum mass of neutron stars
- Conclusions

Nuclear Hamiltonian

Model: non-relativistic nucleons interacting with an effective nucleon-nucleon force (NN) and three-nucleon interaction (TNI).

$$H = -\frac{\hbar^2}{2m}\sum_{i=1}^{A}\nabla_i^2 + \sum_{i<j} v_{ij} + \sum_{i<j<k} V_{ijk}$$

v_{ij} NN fitted on scattering data.

V_{ijk} typically constrained to reproduce light systems (A=3,4).

- "Phenomenological/traditional" interactions (Argonne/Illinois)
- Local chiral forces up to N^2LO (Gezerlis, et al. PRL 111, 032501 (2013), PRC 90, 054323 (2014), Lynn, et al. PRL 116, 062501 (2016)).

Quantum Monte Carlo

Propagation in imaginary time:

$$H\,\psi(\vec{r}_1\ldots\vec{r}_N) = E\,\psi(\vec{r}_1\ldots\vec{r}_N) \qquad \psi(t) = e^{-(H-E_T)t}\psi(0)$$

Ground-state extracted in the limit of $t\to\infty$.

Propagation performed by

$$\psi(R,t) = \langle R|\psi(t)\rangle = \int dR'\,G(R,R',t)\psi(R',0)$$

- Importance sampling: $G(R,R',t) \to G(R,R',t)\,\Psi_I(R')/\Psi_I(R)$
- Constrained-path approximation to control the sign problem. Unconstrained-path calculation possible in several cases (exact).

GFMC includes all spin-states of nucleons in the w.f., nuclei up to A=12
AFDMC samples spin states, bigger systems, less accurate than GFMC

Ground–state obtained in a **non-perturbative way.** Systematic uncertainties within 2-3 %.

See Carlson, et al., Rev. Mod. Phys. 87, 1067 (2015)

Traditional approach (credit D. Furnsthal, T. Papenbrock)

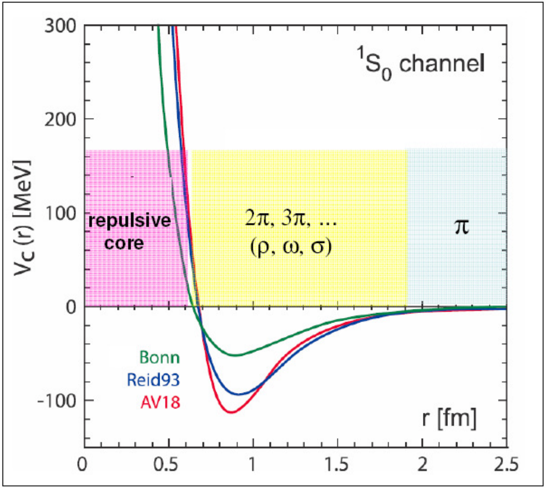

From T. Hatsuda (Oslo 2008)

One-pion exchange by Yukawa (1935)

Multi-pions by Taketani (1951)

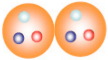

Repulsive core by Jastrow (1951)

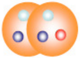

Light nuclei spectrum computed with GFMC

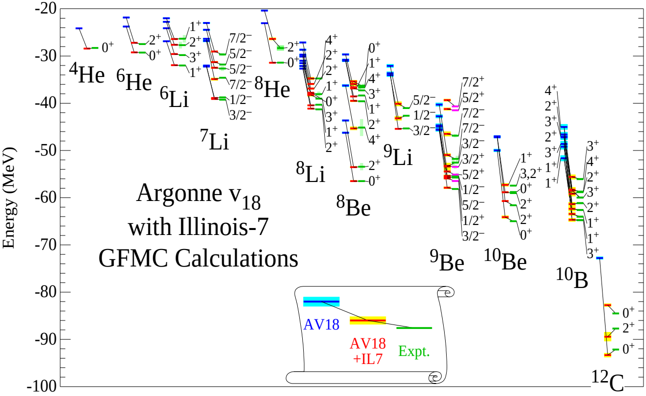

Carlson, et al., Rev. Mod. Phys. 87, 1067 (2015)

Also radii, densities, matrix elements, ...

Unfortunately phenomenological Hamiltonians are not useful to address systematical uncertainties.

Chiral EFT interactions

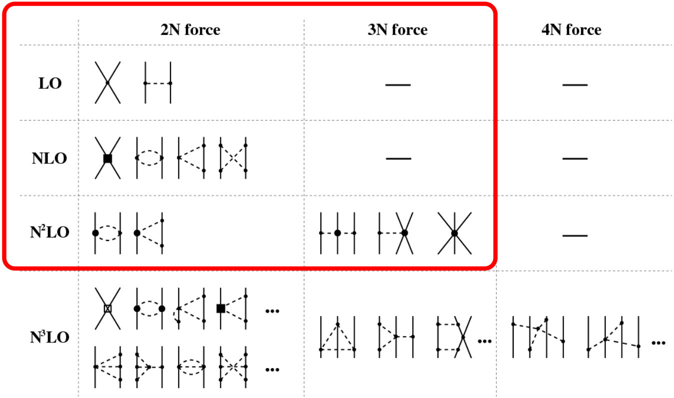

Expansion in powers of Q/Λ, Q$\sim$100 MeV, Λ $\sim$1 GeV.

Long-range physics given by pion-exchanges (no free parameters).

Short-range physics: contact interactions (LECs) to fit.

Operators need to be regulated $\rightarrow$ cutoff dependency!

Order's expansion provides a way to quantify uncertainties!

Truncation error estimate

Error quantification (one possible scheme). Define

$$Q = \max\left(\frac{p}{\Lambda_b}, \frac{m_\pi}{\Lambda_b}\right),$$

where p is a typical nucleon's momentum or k_F for matter, Λ_b is the cutoff, and calculate:

$$\Delta(N2LO) = \max\left(Q^4|\hat{O}_{LO}|,\ Q^2|\hat{O}_{LO} - \hat{O}_{NLO}|,\ Q|\hat{O}_{NLO} - \hat{O}_{N2LO}\right)$$

Epelbaum, Krebs, Meissner (2014).

AFDMC calculations

Energies and charge radii, cutoff 1.0 fm:

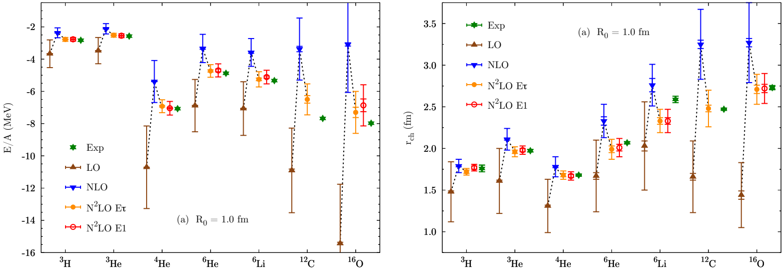

Lonardoni, et al., PRL (2018), PRC (2018).

Qualitative good description of both energies and radii.

Good convergence (although uncertainties still large if LO included).

Neutron matter equation of state

Neutron matter is an "exotic" system. Interesting connections between nuclear structure and neutron stars.

- EOS of neutron matter gives the symmetry energy and its slope.
- The three-neutron force ($T = 3/2$) very weak in light nuclei, while $T = 1/2$ is the dominant part. No direct $T = 3/2$ experiments available.
- Determines radii of neutron stars.

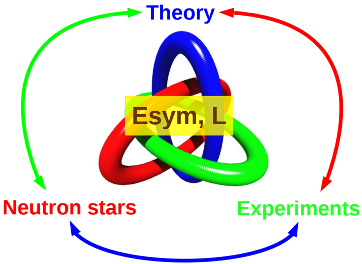

What is the Symmetry energy?

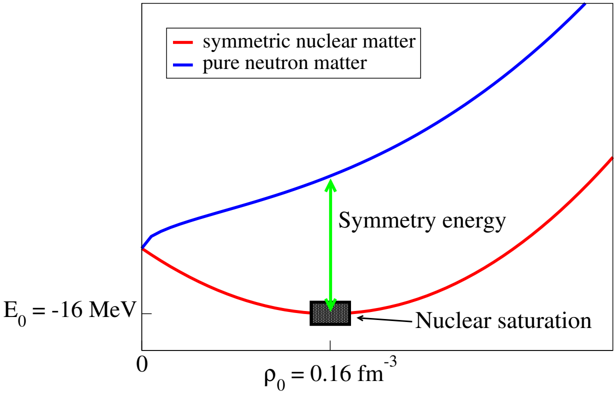

Assumption from experiments:

$$E_{SNM}(\rho_0) = -16 MeV\,, \quad \rho_0 = 0.16 fm^{-3}\,, \quad E_{sym} = E_{PNM}(\rho_0) + 16$$

At ρ_0 we access E_{sym} by studying PNM.

Neutron matter

Equation of state of neutron matter using Argonne/Urbana forces:

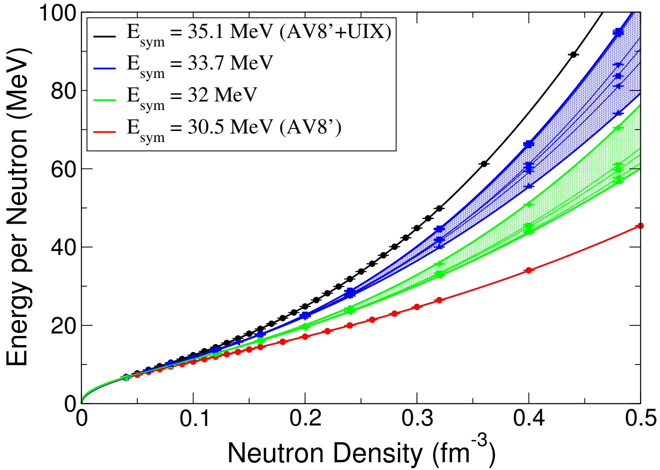

Gandolfi, Carlson, Reddy, PRC (2012)

EOS of pure neutron matter at N2LO, R_0=1.0 fm

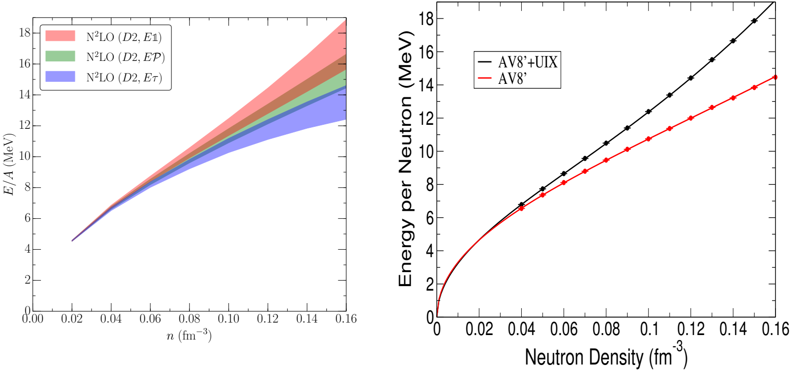

Lynn, Tews, Carlson, Gandolfi, Gezerlis, Schmidt, Schwenk PRL (2016).

Significant dependence to the choice of V_E, but similar results to phenomenological Hamiltonians.

EOS of pure neutron matter at N2LO, R_0=1.0 fm

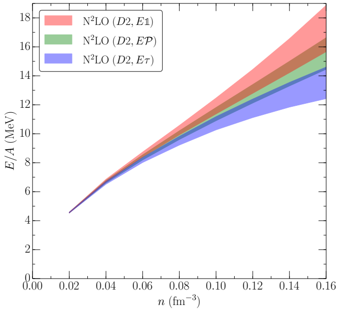

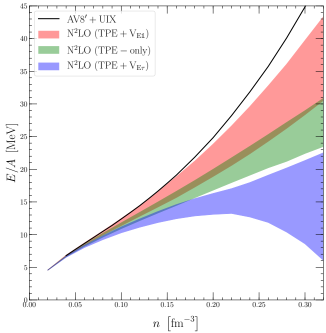

Tews, Carlson, Gandolfi, Reddy, APJ (2018).

Errors grow quickly with the density.

Blue band not even physical!

TOV equations:

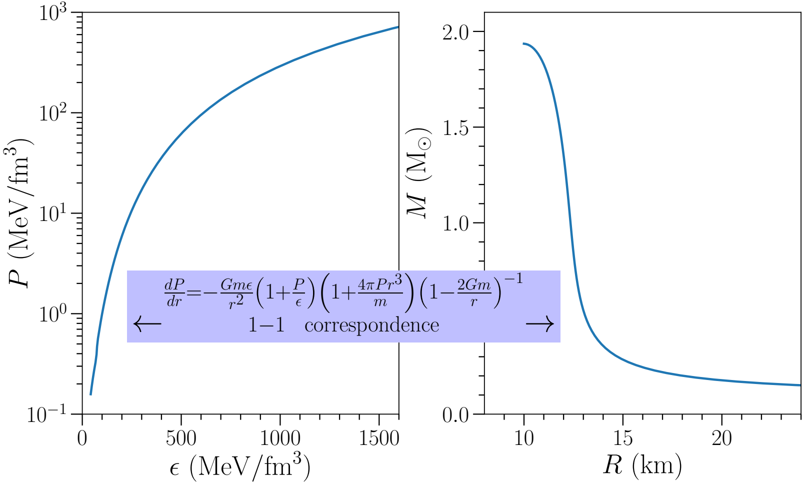

$$\frac{dP}{dr} = -\frac{Gm\epsilon}{r^2}\left(1+\frac{P}{\epsilon}\right)\left(1+\frac{4\pi P r^3}{m}\right)\left(1-\frac{2Gm}{r}\right)^{-1}$$

$\leftarrow$ 1–1 correspondence $\rightarrow$

Neutron star structure

EOS used to solve the TOV equations.

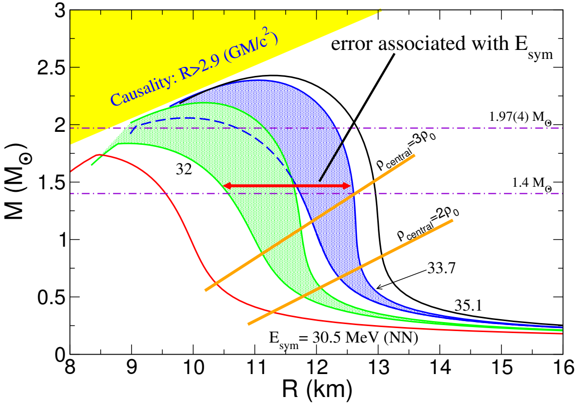

Gandolfi, Carlson, Reddy, PRC (2012).

Accurate measurement of E_{sym} put a constraint to the radius of neutron stars, **OR** observation of M and R would constrain E_{sym}!

Observations of the mass-radius relation are becoming available:

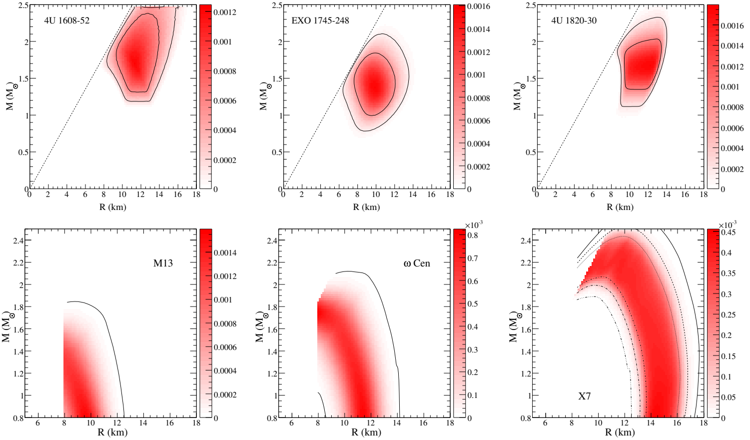

Steiner, Lattimer, Brown, ApJ (2010)

Neutron star observations can be used to 'measure' the EOS and constrain E_{sym} and L. (Systematic uncertainties still under debate...)

Neutron star matter

Neutron star matter model:

$$E_{NSM} = a\left(\frac{\rho}{\rho_0}\right)^{\alpha} + b\left(\frac{\rho}{\rho_0}\right)^{\beta}, \quad \rho < \rho_t$$

form suggested by QMC simulations,
contrast with the commonly used $E_{FG} + V$

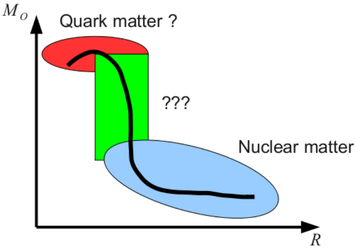

and a high density model for $\rho > \rho_t$

i) two polytropes

ii) polytrope+quark matter model

Neutron star radius sensitive to the EOS at nuclear densities!

Direct way to extract E_{sym} and L from neutron stars observations:

$$E_{sym} = a + b + 16, \quad L = 3(a\alpha + b\beta)$$

Neutron star matter really matters!

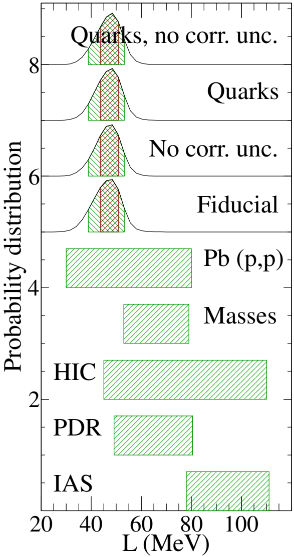

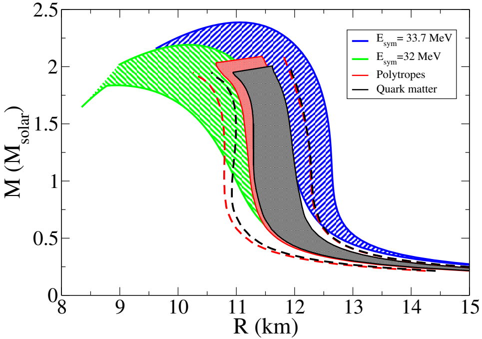

$32 < E_{sym} < 34\ MeV$

$43 < L < 52\ MeV$

Steiner, Gandolfi, PRL (2012).

EOS around nuclear densities (1-2)ρ_0 almost determines radii.

What about higher densities and maximum mass?

Model the EOS at high densities

Speed of sound:

$$c_S^2 = \frac{\partial p(\epsilon)}{\partial \epsilon} ,$$

in the limit of large densities we know that $c_S^2 \to 1/3$:

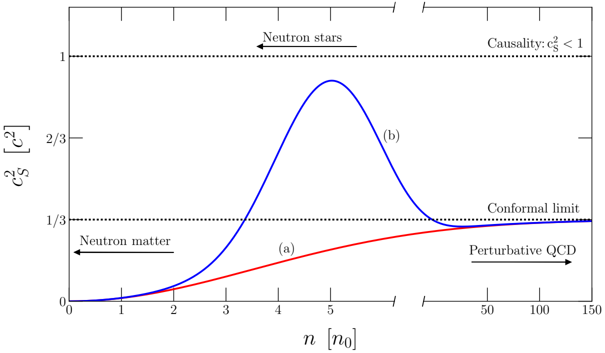

Tews, Carlson, Gandolfi, Reddy, APJ (2018).

Speed of sound of our EOS:

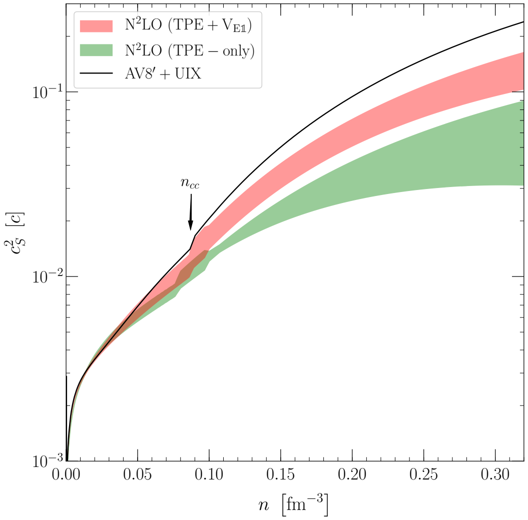

Tews, Carlson, Gandolfi, Reddy, APJ (2018).

Strategy: nuclear EOS up to some density, then parametrize c_S^2.

Sample parameters by requiring maximum mass to be at least 2 solar masses.

Two possibilities: c_S^2 always below the $1/3$ limit, or not.

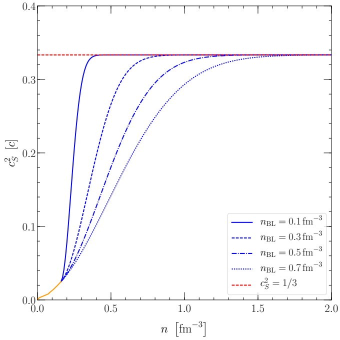

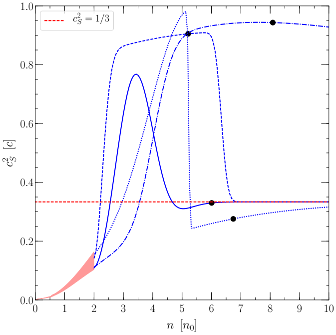

Tews, Carlson, Gandolfi, Reddy, APJ (2018).

EOS with $c_S^2 < 1/3$:

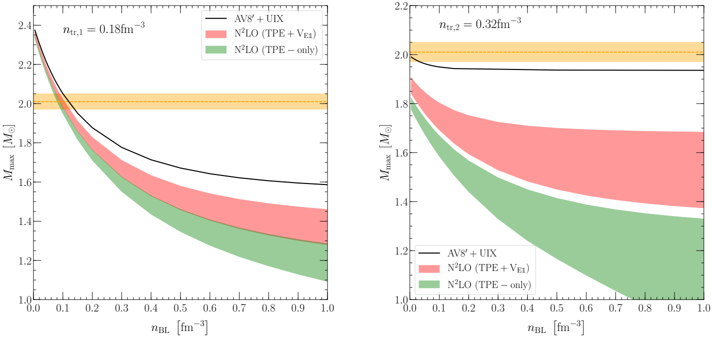

Tews, Carlson, Gandolfi, Reddy, APJ (2018).

By considering nuclear EOS up to $0.16 fm^{-3}$ all the EOS can support 2 solar masses.

If instead up to $0.32 fm^{-3}$ only the stiffer one is barely fine.

Transition density 0.16 fm^{-3}, chiral and AV8'+UIX Hamiltonians. Mass-radius, and EOS:

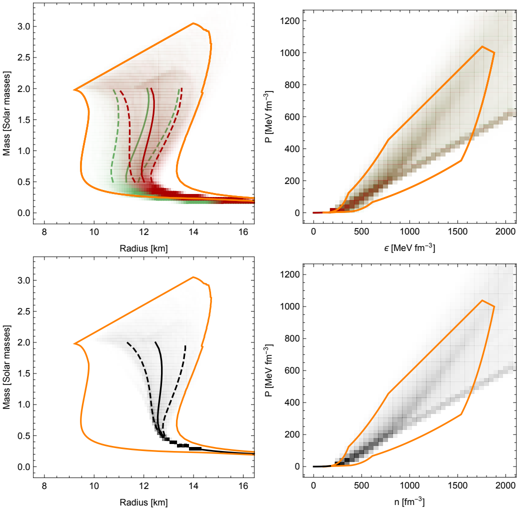

Tews, Carlson, Gandolfi, Reddy, APJ (2018).

Transition density 0.32 fm^{-3}, chiral and AV8'+UIX Hamiltonians. Mass-radius, and EOS:

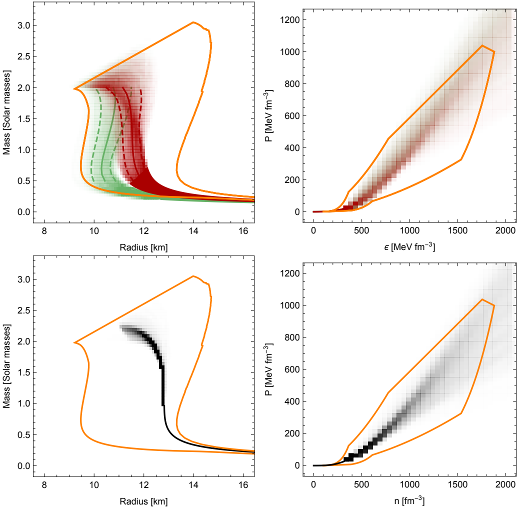

Tews, Carlson, Gandolfi, Reddy, APJ (2018).

Summary

- EOS of pure neutron matter qualitatively well understood
- Nuclear symmetry energy and neutron star radii strongly correlated
- Constraints on the speed of sound of dense matter might strongly constrain the nuclear EOS

Acknowledgments:
J. Carlson (LANL)
I. Tews (LANL)
D. Lonardoni (LANL/FRIB)
S. Reddy (INT/UW)
A. Steiner (UTK)

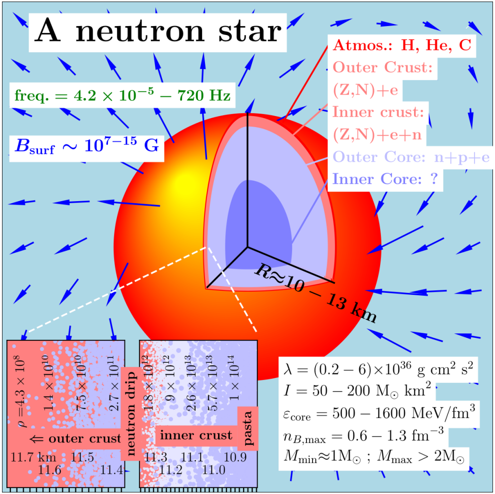

Gandolfi et al., arXiv:1903.06730.

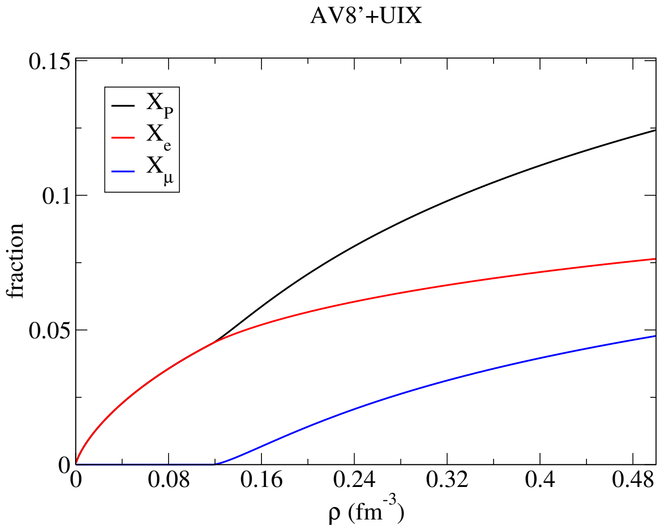

Gandolfi et al., arXiv:1903.06730.

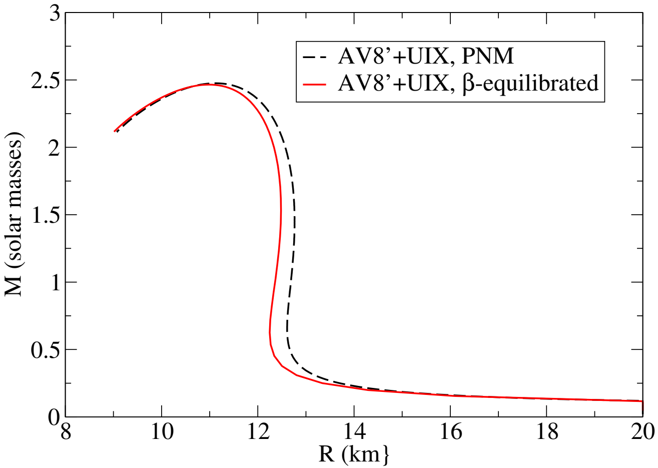

Gandolfi et al., arXiv:1903.06730.

Scattering data and neutron matter

Two neutrons have

$$k \approx \sqrt{E_{lab}\, m/2}\,, \qquad \rightarrow k_F$$

that correspond to

$$k_F \rightarrow \rho \approx (E_{lab}\, m/2)^{3/2}/2\pi^2\,.$$

E_{lab}=150 MeV corresponds to about 0.12 fm^{-3}.

E_{lab}=350 MeV to 0.44 fm^{-3}.

Argonne potentials useful to study dense matter above ρ_0=0.16 fm^{-3}

Nuclei and hypernuclei

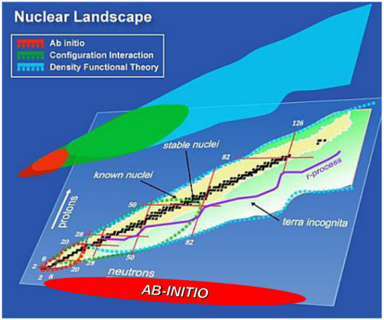

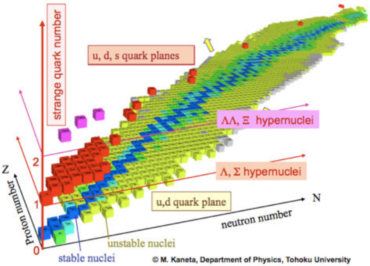

Few thousands of binding energies for normal nuclei are known.

Only few tens for hypernuclei.

High density neutron matter

If chemical potential large enough ($\rho \sim 2 - 3\rho_0$), nucleons produce Λ, Σ, ...

Non-relativistic BHF calculations suggest that available hyperon-nucleon Hamiltonians support an EOS with $M > 2M_\odot$:

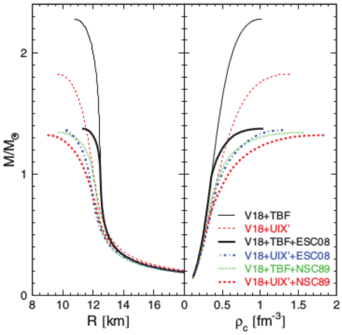

Schulze and Rijken PRC (2011).

Vidana, Logoteta, Providencia, Polls, Bombaci EPL (2011).

Note: (Some) other relativistic model support $2M_\odot$ neutron stars.

$\longrightarrow$ *Hyperon puzzle*

Λ-systems, outline

Λ-hypernuclei and hypermatter

$$H = H_N + \frac{\hbar^2}{2m_\Lambda}\sum_{i=1}^{A}\nabla_i^2 + \sum_{i<j} v_{ij}^{\Lambda N} + \sum_{i<j<k} V_{ijk}^{\Lambda NN}$$

Λ-binding energy calculated as the difference between the system with and without Λ.

Λ-nucleon interaction

The Λ-nucleon interaction is constructed similarly to the Argonne potentials (Usmani).

Argonne NN: $v_{ij} = \sum_p v_p(r_{ij}) O_{ij}^p$, $O_{ij} = (1, \sigma_i \cdot \sigma_j, S_{ij}, \vec{L}_{ij} \cdot \vec{S}_{ij}) \times (1, \tau_i \cdot \tau_j)$

Usmani ΛN: $v_{ij} = \sum_p v_p(r_{ij}) O_{ij}^p$, $O_{\lambda j} = (1, \sigma_\lambda \cdot \sigma_j) \times (1, \tau_j^z)$

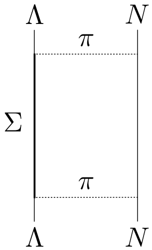

Unfortunately... ∼4500 NN data, ∼30 of ΛN data.

ΛN and ΛNN interactions

ΛNN has the same range of ΛN

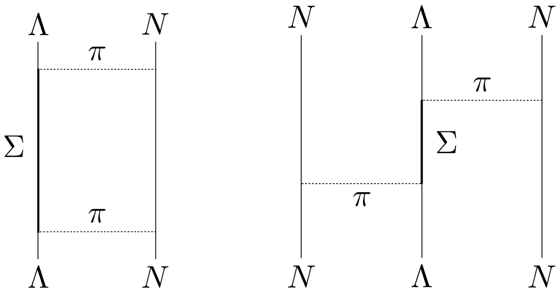

Λ hypernuclei

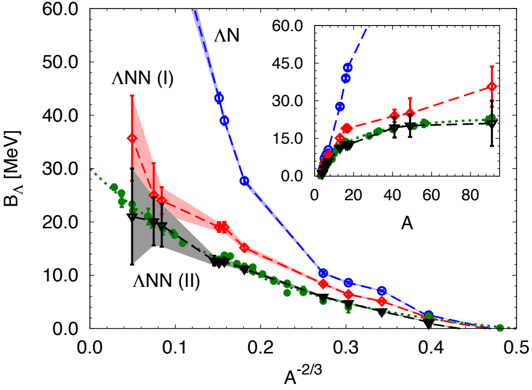

Lonardoni, Gandolfi, Pederiva, PRC (2013) and PRC (2014).

$V^{\Lambda NN}$ (II) is a new form where the parameters have been readjusted.

ΛNN crucial for saturation.

Hyper-neutron matter

Neutrons and Λ particles:

$$\rho = \rho_n + \rho_\Lambda \,, \qquad\qquad x = \frac{\rho_\Lambda}{\rho}$$

$$E_{\rm HNM}(\rho,x) = \Big[E_{\rm PNM}((1-x)\rho)+m_n\Big](1-x)+\Big[E_{\rm P\Lambda M}(x\rho)+m_\Lambda\Big]x+f(\rho,x)$$

where $E_{P\Lambda M}$ is the non-interacting energy (no $v_{\Lambda\Lambda}$ interaction),

$$E_{PNM}(\rho) = a\left(\frac{\rho}{\rho_0}\right)^\alpha + b\left(\frac{\rho}{\rho_0}\right)^\beta$$

and

$$f(\rho,x) = c_1\frac{x(1-x)\rho}{\rho_0} + c_2\frac{x(1-x)^2\rho^2}{\rho_0^2}$$

All the parameters are fit to Quantum Monte Carlo results.

Λ-neutron matter

EOS obtained by solving for $\mu_\Lambda(\rho, x) = \mu_n(\rho, x)$

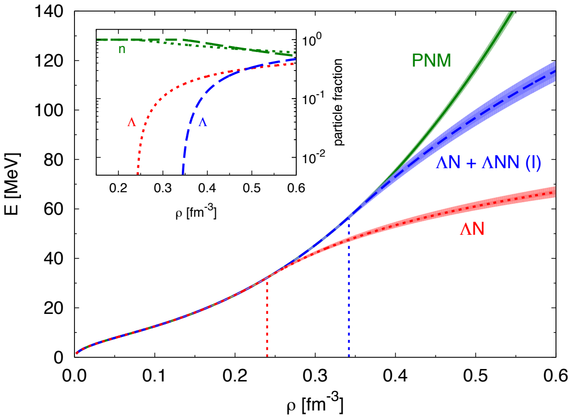

Lonardoni, Lovato, Gandolfi, Pederiva, PRL (2015)

No hyperons up to $\rho = 0.5$ fm^{-3} using ΛNN (II)!!!

Λ-neutron matter

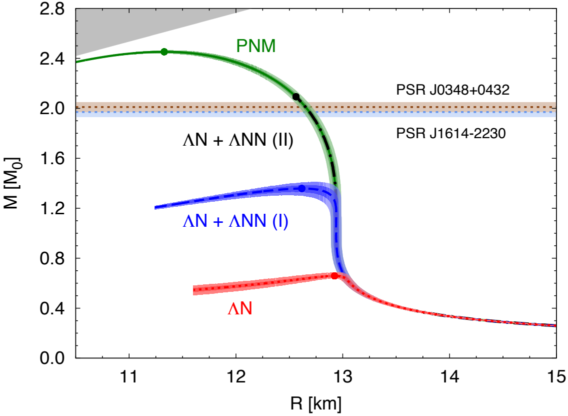

Lonardoni, Lovato, Gandolfi, Pederiva, PRL (2015)

Drastic role played by ΛNN. Calculations can be compatible with neutron star observations.

Note: no $v_{\Lambda\Lambda}$, no protons, and no other hyperons included yet...

Phase shifts, AV8'

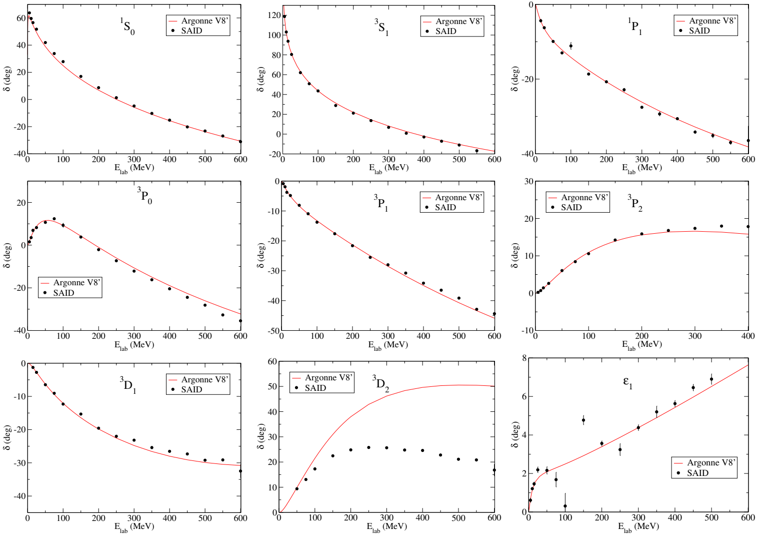

Difference AV8′-AV18 less than 0.2 MeV per nucleon up to A=12.

Phase shifts, LO, NLO and N^2LO with R_0=1.0 and 1.2 fm:

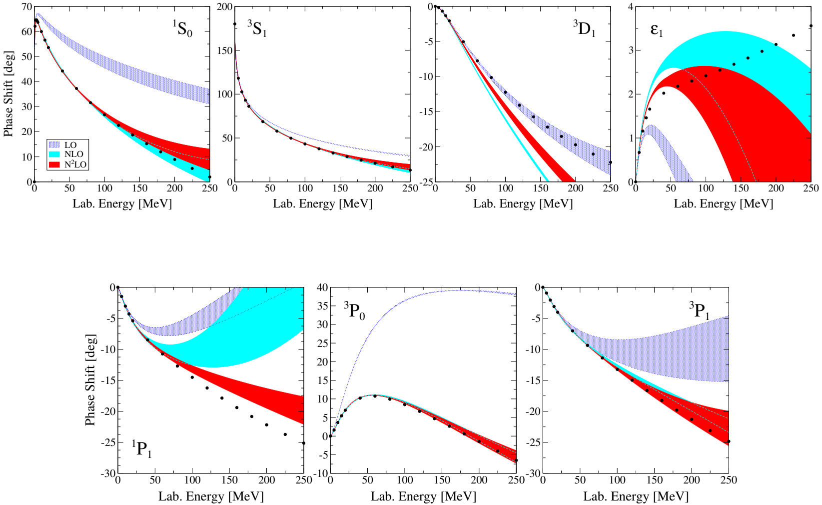

Three-body forces

Urbana–Illinois V_{ijk} models processes like

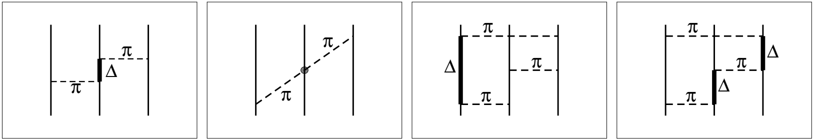

$+$ short-range correlations (spin/isospin independent).

Chiral forces at N^{2}LO:

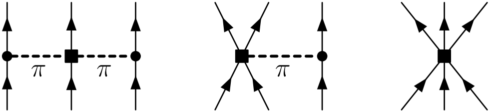

Nuclear Hamiltonians

Advantages:

- Argonne interactions fit phase shifts up to high energies. At $\rho = \rho_0$, $k_F \simeq 330$ MeV. Two neutrons have $E_{CM} \simeq 120$ MeV, $E_{LAB} \simeq 240$ MeV. $\rightarrow$ accurate up to (at least) 2-3ρ_0. Provide a very good description of several observables in light nuclei.
- Interactions derived from chiral EFT can be systematically improved. Changing the cutoff probes the physics and energy scales entering into observables. They are generally softer, and make most of the calculations easier to converge.

Disadvantages:

- Phenomenological interactions are phenomenological, not clear how to improve their quality. Systematic uncertainties hard to quantify.
- Chiral interactions describe low-energy (momentum) physics. How do they work at large momenta, (i.e. e and ν scattering)?

Important to consider both and compare predictions

Quantum Monte Carlo

$$H\,\psi(\vec{r}_1 \ldots \vec{r}_N) = E\,\psi(\vec{r}_1 \ldots \vec{r}_N) \qquad \psi(t) = e^{-(H-E_T)t}\psi(0)$$

Ground-state extracted in the limit of $t \to \infty$.

Propagation performed by

$$\psi(R,t) = \langle R|\psi(t)\rangle = \int dR' G(R,R',t)\psi(R',0)$$

- Importance sampling: $G(R,R',t) \to G(R,R',t)\,\Psi_I(R')/\Psi_I(R)$
- Constrained-path approximation to control the sign problem. Unconstrained calculation possible in several cases (exact).

Ground–state obtained in a **non-perturbative way.** Systematic uncertainties within 1-2 %.

Overview

Recall: propagation in imaginary-time

$$e^{-(T+V)\Delta\tau}\psi \approx e^{-T\Delta\tau}e^{-V\Delta\tau}\psi$$

Kinetic energy is sampled as a diffusion of particles:

$$e^{-\nabla^2\Delta\tau}\psi(R) = e^{-(R-R')^2/2\Delta\tau}\psi(R) = \psi(R')$$

The (scalar) potential gives the weight of the configuration:

$$e^{-V(R)\Delta\tau}\psi(R) = w\psi(R)$$

Algorithm for each time-step:

- do the diffusion: $R' = R + \xi$
- compute the weight w
- compute observables using the configuration R' weighted using w over a trial wave function ψ_T.

For spin-dependent potentials things are much worse!

Branching

The configuration weight w is efficiently sampled using the branching technique:

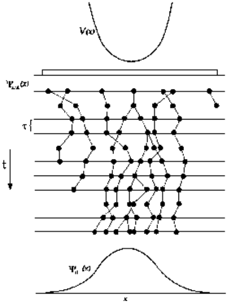

Configurations are replicated or destroyed with probability

$$int[w + \xi]$$

Note: the re-balancing is the bottleneck limiting the parallel efficiency.

GFMC and AFDMC

Because the Hamiltonian is state dependent, all spin/isospin states of nucleons must be included in the wave-function.

Example: spin for 3 neutrons (radial parts also needed in real life):

GFMC wave-function:

$$\psi = \begin{pmatrix} a_{\uparrow\uparrow\uparrow} \\ a_{\uparrow\uparrow\downarrow} \\ a_{\uparrow\downarrow\uparrow} \\ a_{\uparrow\downarrow\downarrow} \\ a_{\downarrow\uparrow\uparrow} \\ a_{\downarrow\uparrow\downarrow} \\ a_{\downarrow\downarrow\uparrow} \\ a_{\downarrow\downarrow\downarrow} \end{pmatrix}$$

A correlation like

$$1 + f(r)\sigma_1 \cdot \sigma_2$$

can be used, and the variational wave function can be very good. Any operator accurately computed.

AFDMC wave-function:

$$\psi = \mathcal{A}\left[\xi_{s_1}\begin{pmatrix} a_1 \\ b_1 \end{pmatrix}\xi_{s_2}\begin{pmatrix} a_2 \\ b_2 \end{pmatrix}\xi_{s_3}\begin{pmatrix} a_3 \\ b_3 \end{pmatrix}\right]$$

We must change the propagator by using the Hubbard-Stratonovich transformation:

$$e^{\frac{1}{2}\Delta t O^2} = \frac{1}{\sqrt{2\pi}}\int dx e^{-\frac{x^2}{2}+x\sqrt{\Delta t}O}$$

Auxiliary fields x must also be sampled.

The wave-function is pretty bad, but we can simulate larger systems (up to $A \approx 100$). Operators (except the energy) are very hard to be computed, but in some case there is some trick!

Propagator

We first rewrite the potential as:

$$V = \sum_{i<j} [v_\sigma(r_{ij})\vec{\sigma}_i \cdot \vec{\sigma}_j + v_t(r_{ij})(3\vec{\sigma}_i \cdot \hat{r}_{ij}\vec{\sigma}_j \cdot \hat{r}_{ij} - \vec{\sigma}_i \cdot \vec{\sigma}_j)] =$$

$$= \sum_{i,j} \sigma_{i\alpha} A_{i\alpha;j\beta} \sigma_{j\beta} = \frac{1}{2}\sum_{n=1}^{3N} O_n^2 \lambda_n$$

where the new operators are

$$O_n = \sum_{j\beta} \sigma_{j\beta} \psi_{n,j\beta}$$

Now we can use the HS transformation to do the propagation:

$$e^{-\Delta\tau \frac{1}{2}\sum_n \lambda O_n^2}\psi = \prod_n \frac{1}{\sqrt{2\pi}} \int dx e^{-\frac{x^2}{2} + \sqrt{-\lambda\Delta\tau} x O_n}\psi$$

Computational cost $\approx (3N)^3$.

Three-body forces

Three-body forces, Urbana, Illinois, and local chiral N^2LO can be exactly included in the case of neutrons.

For example:

$$
\begin{aligned}
O_{2\pi} &= \sum_{cyc}\left[\{X_{ij},X_{jk}\}\{\tau_i\cdot\tau_j,\tau_j\cdot\tau_k\}+\frac{1}{4}[X_{ij},X_{jk}][\tau_i\cdot\tau_j,\tau_j\cdot\tau_k]\right] \\
&= 2\sum_{cyc}\{X_{ij},X_{jk}\}=\sigma_i\sigma_k f(r_i,r_j,r_k)
\end{aligned}
$$

The above form can be included in the AFDMC propagator.

Three-body forces

$$
\begin{aligned}
V_a^{2\pi,PW} &= A_a^{2\pi,PW} \sum_{i<j<k} \sum_{cyc} \{\vec{\tau}_i \cdot \vec{\tau}_k, \vec{\tau}_j \cdot \vec{\tau}_k\}\{\sigma_i^\alpha \sigma_k^\gamma, \sigma_k^\mu \sigma_j^\beta\} \mathcal{X}_{i\alpha k\gamma} \mathcal{X}_{k\mu j\beta} \\
&= 4A_a^{2\pi,PW} \sum_{i<j} \vec{\tau}_i \cdot \vec{\tau}_j \sigma_i^\alpha \sigma_j^\beta \sum_{k\neq i,j} \mathcal{X}_{i\alpha k\gamma} \mathcal{X}_{k\gamma j\beta} \,, \qquad (1)
\end{aligned}
$$

$$
\begin{aligned}
V_c^{2\pi,PW} &= A_c^{2\pi,PW} \sum_{i<j<k} \sum_{cyc} [\vec{\tau}_i \cdot \vec{\tau}_k, \vec{\tau}_j \cdot \vec{\tau}_k][\sigma_i^\alpha \sigma_k^\gamma, \sigma_k^\mu \sigma_j^\beta] \mathcal{X}_{i\alpha k\gamma} \mathcal{X}_{k\mu j\beta} \\
&= -4A_c^{2\pi,PW} \sum_{i<j<k} \sum_{cyc} \tau_i^\eta \tau_j^\xi \tau_k^\phi \epsilon_{\eta\xi\phi} \sigma_i^\alpha \sigma_j^\beta \sigma_k^\nu \epsilon_{\nu\gamma\mu} \mathcal{X}_{i\alpha k\gamma} \mathcal{X}_{k\mu j\beta} \qquad (2) \\
&= A_c^{2\pi,PW} \sum_{i<j<k} \sum_{cyc} [\vec{\tau}_i \cdot \vec{\tau}_k, \vec{\tau}_j \cdot \vec{\tau}_k][\sigma_i^\alpha \sigma_k^\gamma, \sigma_k^\mu \sigma_j^\beta] \left(X_{i\alpha k\gamma} - \delta_{\alpha\gamma} \frac{4\pi}{m_\pi^3} \Delta(r_{ik}) \right) \left(X_{k\mu j\beta} - \delta_{\mu\beta} \frac{4\pi}{m_\pi^3} \Delta(r_{kj}) \right) \qquad (3) \\
&= V_c^{\Delta\Delta} + V_c^{\Delta\delta} + V_c^{\delta\delta} \qquad (4)
\end{aligned}
$$

$$
\begin{aligned}
V^{2\pi,SW} &= A^{2\pi,SW} \sum_{i<j<k} \sum_{cyc} \mathcal{Z}_{ik\alpha} \mathcal{Z}_{jk\alpha} \sigma_i^\alpha \sigma_j^\beta \vec{\tau}_i \cdot \vec{\tau}_j \\
&= A^{2\pi,SW} \sum_{i<j} \sigma_i^\alpha \sigma_j^\beta \vec{\tau}_i \cdot \vec{\tau}_j \sum_{k\neq i,j} \mathcal{Z}_{ik\alpha} \mathcal{Z}_{jk\alpha} \qquad (5)
\end{aligned}
$$

$$
V_D = A_D \sum_{i<j} \sigma_i^\alpha \sigma_j^\beta \vec{\tau}_i \cdot \vec{\tau}_j \sum_{k\neq i,j} \mathcal{X}_{i\alpha j\beta} [\Delta(r_{ik}) + \Delta(r_{jk})] \qquad (6)
$$

$$
V_E = A_E \sum_{i<j} \vec{\tau}_i \cdot \vec{\tau}_j \sum_{k\neq i,j} \Delta(r_{ik}) \Delta(r_{jk}) \qquad (7)
$$

Three-body forces

$$H' = H - V_c^{2\pi,PW} + \alpha_1 V_a^{2\pi,PW} + \alpha_2 V_D + \alpha_3 V_E \,. \tag{8}$$

The Hamiltonian H' can be exactly included in the AFDMC propagation. The three constants α_i are adjusted in order to have:

$$\begin{aligned} \langle V_c^{\Delta\Delta} \rangle &\approx \langle \alpha_1 V_a^{2\pi,PW} \rangle \\ \langle V_c^{\Delta\delta} \rangle &\approx \langle \alpha_2 V_D \rangle \\ \langle V_c^{\delta\delta} \rangle &\approx \langle \alpha_3 V_E \rangle \end{aligned} \tag{9}$$

Once the ground state Ψ of H' is calculated with AFDMC as explained above, the expectation value of the Hamiltonian H is given by

$$\begin{aligned} \langle H \rangle &= \langle \Psi | H' | \Psi \rangle + \langle \Psi | H - H' | \Psi \rangle \\ &= \langle \Psi | H' | \Psi \rangle + \langle \Psi | V_c^{2\pi,PW} - \alpha_1 V_a^{2\pi,PW} - \alpha_2 V_D - \alpha_3 V_E | \Psi \rangle \end{aligned} \tag{10}$$

Variational wave function

$$E_0 \leq E = \frac{\langle\psi|H|\psi\rangle}{\langle\psi|\psi\rangle} = \frac{\int dr_1 \ldots dr_N \, \psi^*(r_1 \ldots r_N) H \psi^*(r_1 \ldots r_N)}{\int dr_1 \ldots dr_N \, \psi^*(r_1 \ldots r_N) \psi^*(r_1 \ldots r_N)}$$

$\rightarrow$ Monte Carlo integration. Variational wave function:

$$|\Psi_T\rangle = \left[\prod_{i<j} f_c(r_{ij})\right] \left[\prod_{i<j<k} f_c(r_{ijk})\right] \left[1 + \sum_{i<j,p} \prod_k u_{ijk} f_p(r_{ij}) O^p_{ij}\right] |\Phi\rangle$$

where O^p are spin/isospin operators, f_c, u_{ijk} and f_p are obtained by minimizing the energy. About 30 parameters to optimize.

$|\Phi\rangle$ is a mean-field component, usually HF. Sum of many Slater determinants needed for open-shell configurations.

BCS correlations can be included using a Pfaffian.

Variational wave function

$$\langle RS|\Psi_V\rangle = \langle RS|\left[\prod_{i<j} f^c(r_{ij})\right]\left[1+\sum_{i<j} F_{ij} + \sum_{i<j<k} F_{ijk}\right]|\Phi_{JM}\rangle\,,$$

$$\langle RS|\Phi_{JM}\rangle = \sum_n k_n \left[\sum D\{\phi_\alpha(r_i,s_i)\}\right]_{JM}\,,$$

$$\phi_\alpha(r_i,s_i) = \Phi_{nlj}(r_i)\left[Y_{lm_l}(\hat{r}_i)\xi_{sm_s}(s_i)\right]_{jm_j}\,,$$

In particular, we included orbitals in $1\mathrm{S}_{1/2}$, $1\mathrm{P}_{3/2}$, $1\mathrm{P}_{1/2}$, $1\mathrm{D}_{5/2}$, $2\mathrm{S}_{1/2}$, and $1\mathrm{D}_{3/2}$.

The Sign problem in one slide

Evolution in imaginary-time:

$$\psi_I(R')\Psi(R',t+dt) = \int dR\, G(R,R',dt)\frac{\psi_I(R')}{\psi_I(R)}\psi_I(R)\Psi(R,t)$$

note: $\Psi(R,t)$ must be positive to be "Monte Carlo" meaningful.

Fixed-node approximation: solve the problem in a restricted space where $\Psi > 0$ (Bosonic problem) $\Rightarrow$ upperbound.

If Ψ is complex:

$$|\psi_I(R')||\Psi(R',t+dt)| = \int dR\, G(R,R',dt)\left|\frac{\psi_I(R')}{\psi_I(R)}\right||\psi_I(R)||\Psi(R,t)|$$

Constrained-path approximation: project the wave-function to the real axis. Extra weight given by $\cos\Delta\theta$ (phase of $\frac{\Psi(R')}{\Psi(R)}$), $Re\{\Psi\} > 0 \Rightarrow$ not necessarily an upperbound.

Unconstrained-path

GFMC unconstrained-path propagation:

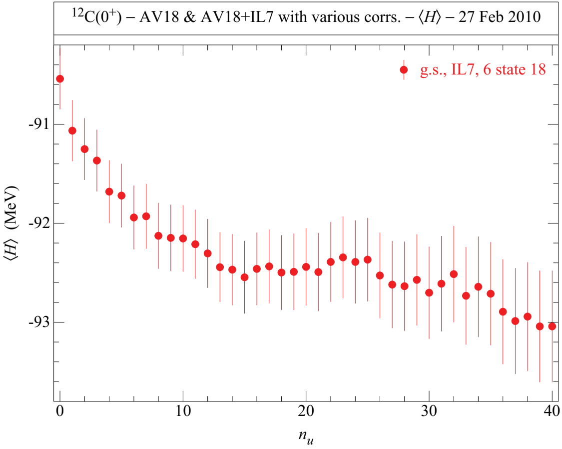

Changing the trial wave function gives same results.

AFDMC unconstrained-path propagation:

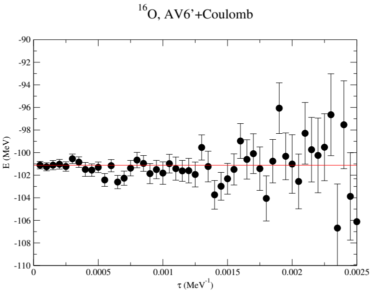

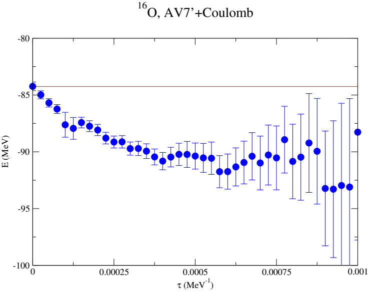

The difference between CP and UP results is mainly due to the presence of LS terms in the Hamiltonian. Same for heavier systems.

Work in progress to improve Ψ to improve the constrained-path.